XH/π (X = C, Si) Interactions in Graphene and Silicene: Weak in Strength, Strong in Tuning Band Structures

ARTICLE *in* JOURNAL OF PHYSICAL CHEMISTRY LETTERS · DECEMBER 2012

Impact Factor: 7.46 · DOI: 10.1021/jz301821n

2 AUTHORS:

Yafei Li
Nanjing Normal University
48 PUBLICATIONS **2,047** CITATIONS
SEE PROFILE

Zhongfang Chen
University of Puerto Rico at Rio Piedras
221 PUBLICATIONS **8,040** CITATIONS
SEE PROFILE

THE JOURNAL OF PHYSICAL CHEMISTRY Letters

Letter

pubs.acs.org/JPCL

XH/π (X = C, Si) Interactions in Graphene and Silicene: Weak in Strength, Strong in Tuning Band Structures

Yafei Li and Zhongfang Chen*

Department of Chemistry, Institute for Functional Nanomaterials, University of Puerto Rico, Rio Piedras Campus, San Juan, Puerto Rico 00931

Supporting Information

ABSTRACT: The lack of a band gap has greatly hindered the applications of graphene in electronic devices. By means of dispersion-corrected density functional theory computations, we demonstrated that considerable CH/π interactions exist between graphene and its fully (graphane) or patterned partially (C_4H) hydrogenated derivatives. Due to the equivalence breaking of two sublattices of graphene, a 90 meV band gap is opened in the graphene/C_4H bilayer. The band gap can be further increased to 270 meV by sandwiching graphene between two C_4H layers. By taking advantage of the similar SiH/π interactions, a 120 meV band gap also can be opened for silicene. Interestingly, the high carrier mobility of graphene/silicene can be well-preserved. Our theoretical results suggest a rather practical solution for gap opening of graphene and silicene, which would allow them to serve as field effect transistors and other nanodevices.

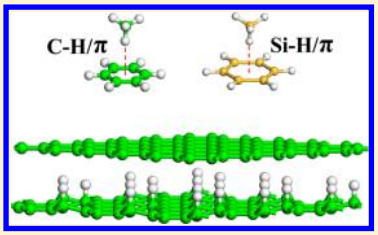

SECTION: Molecular Structure, Quantum Chemistry, and General Theory

In recent years, the importance of noncovalent interactions in condensed matter physics, chemistry, and biology has been gradually recognized.[1−5] Among various noncovalent interactions, the CH/π interaction,[6] which is defined as the weak attractive interaction between the C−H bond of an alkyl or aryl group and the π system (e.g., aromatic ring), is particularly interesting due to its important role in crystal packing,[7,8] molecular recognition,[9,10] chemical reactions,[11,12] and structures of biological molecules.[13−15] The study of CH/π interactions has been very difficult for a rather long time due to their weak strength (0.5−2.5 kcal/mol) and low directionality.[16] The remarkable development of experimental technologies and theoretical methods made it possible to carefully examine the CH/π interactions in the past decade.[17−21] Typically, a CH/π interaction is featured with a C−H bond pointing toward the center of an aromatic ring.[22] Due to the structural similarity, CH/π interactions were once considered as the weakest class of hydrogen bonds. However, high-level ab initio computations[17,18] revealed that the attraction of CH/π interactions is mainly contributed to the dispersion interaction, rather than the electrostatic interaction. Thus, the nature of CH/π interactions is essentially different from hydrogen bonds but close to that of van der Waals (vdW) interactions.

Even several years ago, it was thought that a strictly two-dimensional crystal is physically impossible due to the existence of thermodynamic fluctuation; the successful isolation of graphene in 2004[23] totally refreshed our minds. Ever since, graphene has been intensively studied[24,25] and its many unique properties, such as the Dirac fermions behavior of carriers,[26] quantum hall effect,[27] and ultrahigh Young's modulus,[28] have been demonstrated experimentally. These properties endow graphene many promising applications in many fields.[24] Especially, with ultrafast carrier mobility,[29] graphene is believed to spell the end for silicon and change the future of chips and other microelectronics devices.[30] However, pristine graphene does have an Achilles heel; it is semimetallic and lacks the necessary band gap to turn off the electric current completely, which would disqualify graphene to serve as a transistor. To open a gap in the band structure of graphene, many approaches, such as uniaxial strain[31] and external electronic field,[32] have been applied. Another strategy for this purpose is to convert the sp^2-hybridized carbon atoms in graphene to sp^3-hybridized via hydrogenation. Both experimental[33,34] and theoretical studies[35−39] demonstrated that band gaps can be opened in the fully or partially hydrogenated graphene. However, band gaps opened by hydrogenation are usually too large for practical applications, and tuning carbon atoms to sp^3 hybridization would significantly decrease the carrier mobility of graphene.

Recently, the weak interactions in graphene-related materials began to catch attention. By means of dispersion-corrected density functional theory (DFT) B97D computations, Fokin et al.[40] revealed the strong σ/σ bonding between graphane layers, which is comparable to the π/π interactions in graphene layers; Janowski et al.[41] confirmed the strong σ-stacking, though the strength is a little weaker than π-stacking at the more rigorous CCSD(T) level. Li et al.[42] demonstrated that there exists considerable C−H···F−C bonding between graphane and fluorographene layers, and more interestingly, the graphane/fluorographene bilayer has a band gap (0.5 eV) much lower than those of individual graphane and fluorographene. These

Received: November 8, 2012
Accepted: December 26, 2012

   dx.doi.org/10.1021/jz301821n | J. Phys. Chem. Lett. 2013, 4, 269−275

studies inspired us to answer some interesting questions; because graphene is a π system and (either fully or partially) hydrogenated graphene has C−H bonds, can we pair a graphene layer and a hydrogenated graphene layer together through CH/π interactions? If yes, can we take advantage of CH/π interactions to open a gap in the band structure of graphene while preserving its desired high carrier mobility? To our best knowledge, there has been no attempt to use such a kind of weak interaction to tune the electronic properties of graphene or related materials.

In this work, by means of dispersion-corrected DFT computations, we demonstrated that there truly exist considerable CH/π interactions between graphene and fully hydrogenated (graphane) or patterned partially hydrogenated (C_4H) graphene layers. For the graphene/graphane bilayer, no band gap is opened because the two sublattices of graphene remain equivalent under the CH/π interactions. In contrast, for a graphene/C_4H bilayer, a considerable band gap (90 meV) is opened due to the inversion symmetry breaking. Especially, the band gap of graphene can be further enlarged to 270 meV if it is sandwiched between two C_4H layers. By taking advantage of the similar SiH/π interactions, a 120 meV band gap can also be opened for two-dimensional (2D) silicene. In particular, the desired high carrier mobility of graphene/silicene can be well-preserved.

We constructed the 2D graphene/graphane and graphene/C_4H bilayers by attaching a graphene layer and a graphane or C_4H layer together. For graphane, we adopted the energetically most favorable chair conformation;[36] for the C_4H layer, hydrogen atoms are all adsorbed on one side and arranged in a para-type chemisorption pattern.[34,39] The computed lattice parameters of graphene (2.46 Å), graphane (2.54 Å), and C_4H (4.98 Å) layers are consistent with those of previous studies.[36,39] To simulate the graphene/C_4H bilayer, a 2 × 2 supercell of graphene was used to match the 1 × 1 unit cell of C_4H layer. The optimized lattice parameters for the graphene/graphane and graphene/C_4H bilayers were 2.49 and 4.95 Å, respectively; thus, a small biaxial strain is imposed on graphene in both bilayers. However, our test computations confirmed that the electronic properties of graphene would not be affected by the homogeneous biaxial strain because the inversion symmetry is still kept. We also considered other matching procedures, such as imposing on graphene (graphane) the same lattice parameter as that for graphane (graphene), and found no noticeable differences for the binding energies and electronic properties.

Figure 1 presents the thermodynamically most favorable structures of graphene/graphane and graphene/C_4H bilayers. For the graphene/graphane bilayer, the carbon skeletons are in AB stacking, and C−H bonds of graphane point straight to the center of the aromatic rings of graphene, the same as in a typical CH/π interaction.[22] For the graphene/C_4H bilayer, the carbon skeletons also have the AB stacking feature, and in one unit cell, two C−H bonds of the C_4H layer point to an aromatic ring center and a carbon atom of graphene, respectively. The graphene/graphane bilayer has a equilibrium interlayer distance of 3.54 Å, and its binding energy (112 meV/unit cell) is only slightly smaller than that of the graphene bilayer (132 meV/unit cell), indicating that the strength of the CH/π interactions is comparable to that of π/π interactions, and we can pair a graphene layer and a graphane layer together via CH/π interactions.

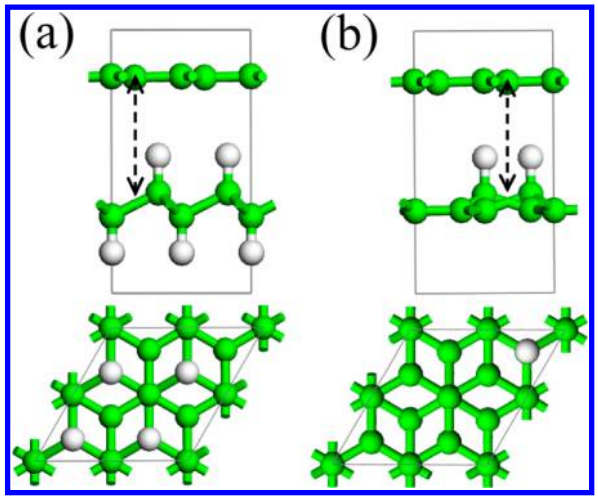

Figure 1. Side (upper) and top (bottom) views of geometric structures of graphene/graphane in a 2 × 2 supercell (a) and graphene/C_4H bilayers in a 1 × 1 unit cell (b). Green and white balls represent carbon and hydrogen atoms, respectively. The black double arrow denotes the equilibrium interlayer distance.

The binding energy of the graphene/C_4H bilayer is 417 meV/unit cell, with a 3.44 Å equilibrium interlayer distance. Note that the unhydrogenated carbon atoms of the C_4H layer are all in aromatic rings;[34,39] thus, besides CH/π interactions, there are also π/π interactions in the graphene/C_4H bilayer, which contribute to the stability of the whole system. According to the Mulliken charge analysis, there is only 0.010 and 0.015 | el/unit cell of charge transfer from graphane and C_4H to graphene, respectively, indicating that the CH/π interactions are mainly of vdW interactions.

To reveal the effect of CH/π interactions on the electronic properties of graphene, we computed the band structures of graphene/graphane and graphene/C_4H bilayers. For comparison, the band structures of graphene, graphane, and C_4H layers were also computed (Figure S1, Supporting Information). For the graphene/graphane bilayer, the π and π^* bands of graphene still touch each other at the K point (Figure 2a). However, the

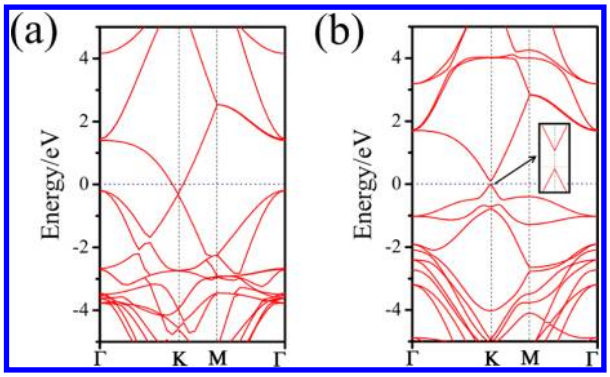

Figure 2. Band structures of graphene/graphane (a) and graphene/C_4H (b) bilayers.

original empty π^* band becomes partially occupied and drops below the Fermi level, which gives rise to the metallization of the graphene/graphane bilayer. In sharp contrast, in the band structure of the graphene/C_4H bilayer (Figure 2b), although the Dirac cone can still be observed, a 90 meV band gap is opened at the K point (as shown in the enlarged inset). The

dx.doi.org/10.1021/jz301821n | J. Phys. Chem. Lett. 2013, 4, 269−275

value of the band gap is much pronounced than the room-temperature thermal voltage (k_BT = 26 meV), implying that the current on/off ratio of the graphene/C_4H bilayer could be significantly increased compared with that of free-standing graphene. Also, the band gap of the graphene/C_4H bilayer is more pronounced than other vdW-interaction-dominated composites, such as graphene/BN[43] and graphene/C_3N_4.[44]

After establishing that a considerable energy gap can be opened in the band structure of the graphene/C_4H bilayer by CH/π interactions, we investigated whether the high carrier mobility of graphene can be preserved. First, we computed the effective mass of the electron (m_e) and hole (m_h) in the valence and conduction bands of the graphene/C_4H bilayer at the K point along the K−M and the K−Γ directions. Here, m_e and m_h are defined as

$$m = \hbar^2\left[\frac{d^2E(k)}{dk^2}\right]^{-1}$$

where $\hbar$ is the reduced Planck constant, k is the wave vector, and $E(k)$ is the dispersion relation. For the graphene/C_4H bilayer, the effective masses of the electron and hole were computed to be $m_e^{KM} = 0.017m_0$, $m_e^{KT} = 0.021m_0$, $m_h^{KM} = 0.016m_0$, and $m_h^{KT} = 0.020m_0$ (m_0 is the free electron mass). On the basis of the simple relationship between carrier mobility (μ) and effective mass (m), $\mu = e\tau/m$, where τ is the scattering time (10^{-13} s for graphene), we can estimate the carrier mobility of the graphene/C_4H bilayer to be on the order of 10^4 cm^2 V^{-1} S^{-1}. Though this value is lower than that of suspended graphene (2×10^5 cm^2 V^{-1} S^{-1}),[23] it is close to the experimentally observed values of single and bilayer graphene on substrates.[45] Therefore, pairing the C_4H layer on graphene can open a considerable band gap without sacrificing the desired high carrier mobility.

Here, a question arises; why does the graphene/C_4H bilayer have a band gap whereas the graphene/graphane bilayer is metallic? To address this question, we carefully checked the charge population of the graphene layer in both bilayers. In the graphene/graphane bilayer, the carbon atoms of graphene uniformly possess −0.005 |e| of charge. In contrast, in the graphene/C_4H bilayer, the notable charge redistribution happens in the graphene layer, which makes the charge populations of any two neighboring carbon atoms different (Figure S2, Supporting Information). Therefore, the two sublattices of graphene in the graphene/graphane bilayer still remain equivalent, while the equivalence in the graphene/C_4H bilayer is broken. It is not difficult to understand because the carbon atoms of graphene in the graphene/graphane bilayer are equivalently affected by CH/π interactions while those in the graphene/C_4H bilayer are not. According to the π-electron tight binding theory, the energy level dispersion of graphene near the Fermi level can be approximated as

$$E(k) = \pm\sqrt{\Delta^2 + (\hbar\nu_F k)^2}$$

where k is the wave vector relative to the K points, ν_F is the Fermi velocity, and Δ is the onsite energy difference between the two sublattices.[46] The +/− correspond to conduction and valence bands, respectively. For free-standing graphene and graphene in the graphene/graphane bilayer, the two sublattices remain equivalent; hence, $\Delta = 0$, resulting in a zero band gap at the K point ($k = 0$); for graphene in the graphene/C_4H bilayer, the equivalence of two sublattices is broken, and $\Delta \neq 0$, yielding a nonzero band gap ($E_g = 2\Delta$) at the K point. In a recent theoretical study, Zhu et al.[47] also revealed that a zero-gap band structure of graphene can be well-preserved when sealed between hydrogen-terminated diamond films because the inversion symmetry is not broken. In light of the above analysis, we can conclude that band gap opening of the graphene/C_4H bilayer is essentially due to the equivalence breaking of two sublattices of graphene induced by CH/π interactions.

Is it possible to further enlarge the band gap of graphene via CH/π interactions? Theoretically, it could be achieved by breaking the equivalence of two sublattices more decidedly. Along this line, we sandwiched graphene between two C_4H layers. As shown in Figure 3a, three carbon skeletons are in

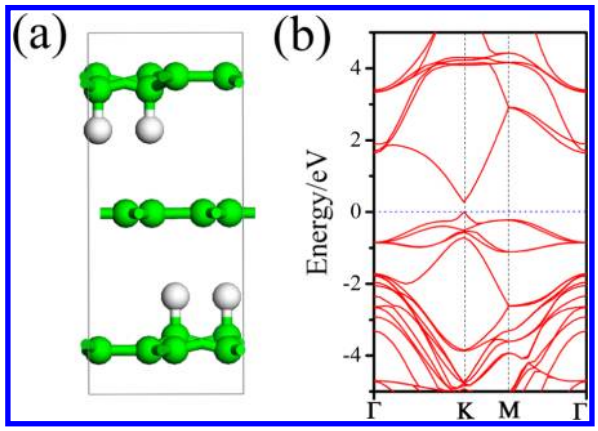

Figure 3. Geometric structure and band structure of the C_4H/graphene/C_4H trilayer.

ABA stacking, and C−H bonds of two C_4H layers point to different aromatic rings and carbon atoms, respectively. The equilibrium distances between the graphene layer and two C_4H layers are both 3.45 Å, with an average binding energy of 412 meV/unit cell. Sandwiching graphene between two C_4H layers further increases the inequivalence of the two sublattices, as denoted by the charge population analysis (Figure S2, Supporting Information). As a result, the band gap of the C_4H/graphene/C_4H trilayer is enlarged to 270 meV (Figure 3b). The effective carrier masses of the C_4H/graphene/C_4H trilayer ($m_e^{KM} = 0.023m_0$, $m_e^{KT} = 0.030m_0$, $m_h^{KM} = 0.020m_0$, and $m_h^{KT} = 0.024m_0$) are a little higher than those of the graphene/C_4H bilayer, indicating that the carrier mobility is still on the order of 10^4 cm^2 V^{-1} S^{-1}.

The remarkable effect of CH/π interactions on tuning the electronic properties of graphene reminds us of another 2D material, silicene,[48] which is a structural analogue of graphene. Recently, silicene has been experimentally realized by depositing Si atoms on the Ag substrates.[49−52] The hydrogenated silicene (silicane), which is known as layered polysilane, was experimentally realized even before silicene was synthesized.[53−55] Theoretical studies[56,57] demonstrated that electronic properties of silicene are quite close to those of graphene; the π and π^* bands at the Fermi level are linear, and hence, the charge carries are also massless. Especially, silicene can be more easily integrated into current Si-based electronics devices compared with graphene. However, silicene is also semimetallic like graphene, which essentially hurdles its application in field effect transistors. The band gap opening of graphene by CH/π interactions makes us wonder if it is

dx.doi.org/10.1021/jz301821n | J. Phys. Chem. Lett. 2013, 4, 269−275

possible to open a band gap for silicene via the SiH/π interactions.

Figure 4a presents the geometric structure of the silicene/silicane bilayer in the most stable stacking pattern. For silicane,

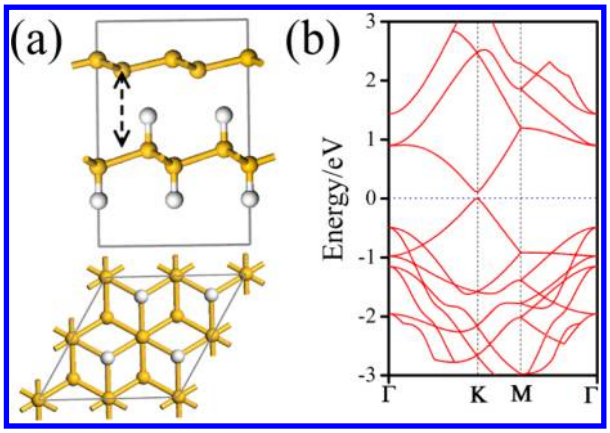

Figure 4. (a) Side (upper) and top (bottom) views of the optimized silicene/silicane bilayer in a 2 × 2 supercell. Yellow and white balls represent silicon and hydrogen atoms, respectively. (b) Band structure of the silicene/silicane bilayer.

we adopted the energetically most favorable chair conformation.[58−60] Note that the structure of silicene is a little buckled, rather than purely planar like graphene.[56] The lattice parameter of silicane (3.87 Å) is the same as that of silicene. In the silicene/silicane bilayer, the silicon skeletons are in AB stacking, and Si−H bonds of silicane point to the center of the silicene hexagons. The binding energy of the silicene/silicene bilayer (159 meV/unit cell) indicates that strong SiH/π interactions exist between silicene and silicane layers. The equilibrium interlayer distance is 3.55 Å, and there is about 0.01 |e| of charge transfer from the silicane layer to the silicene layer.

Excitingly, the silicene/silicane bilayer has a 120 meV band gap, which is even larger than that of the graphene/C_4H bilayer. For comparison, silicene and silicane are semimetallic and semiconducting with a 2.52 eV band gap (Figure S3, Supporting Information), respectively. According to a recent theoretical study,[61] opening a 120 meV band gap for silicene requires a strong external electronic field of 0.75 V/Å, which is experimentally rather challenging. Our results demonstrate that it is rather feasible to open a considerable band gap for silicene via weak nonbonding interactions.

We also estimated the carrier mobility of the silicene/silicane bilayer. The effective carrier masses of the silicene/silicane bilayer were computed to be $m_e^{KM} = 0.022m_0$, $m_e^{KT} = 0.017m_0$, $m_h^{KM} = 0.021m_0$, and $m_h^{KT} = 0.017m_0$. Assuming that silicene has the same scattering time (τ) as graphene, the carrier mobility of silicene/silicane is estimated to be also in the order of 10^4 cm^2 V^{-1} S^{-1}, which is much higher than that of silicon bulk.

With similar structural properties, why does the silicene/silicane bilayer have a band gap while the graphene/graphane bilayer is metallic? This is because silicene prefers a low-buckled structure rather than planar; [56] therefore, the atoms in silicene are no longer equivalently affected by SiH/π interactions. The population analysis reveals that silicon atoms of two sublattices are charged with 0.06 |e| and −0.07 |e|, respectively. Obviously, SiH/π interactions lead to the charge redistribution of the silicene layer and hence break the equivalence of two sublattices, resulting in a considerable band gap.

To summarize, comprehensive theoretical computations revealed notable XH/π (X = C, Si) interactions between 2D graphene or silicene and their hydrogenated phases. Due to the equivalence breaking of two sublattices inducted by XH/π (X = C, Si) interactions, considerable band gaps can be opened in the band structures of graphene/C_4H and silicene/silicane bilayers. These results provide a practical approach for gap opening of graphene and silicene while well preserving their high carrier mobility, which would pave the way for their applications in nanoelectronics. In view of the remarkable experimental progress on controlled synthesis of graphene-related materials, we are rather optimistic that our theoretical proposal can be realized by experimental peers soon.

■ COMPUTATIONAL DETAILS

The computations employed an all-electron method within a generalized gradient approximation (GGA) for the exchange−correlation term, as implemented in the DMol^3 code.[62,63] The double numerical plus polarization (DNP) basis set and PBE[64] functional were adopted. Because the weak interactions are not well described by the standard PBE functional, we adopted a PBE-D2 (D stands for dispersion) approach with the Grimme vdW correction.[65] This approach is a hybrid semiempirical solution that introduces damped atom-pairwise dispersion correction of the form C_6R^{-6} in the DFT formalism. As a benchmark, the binding energy of graphite (64 meV/atom) computed using the PBE-D2 method is quite close to the experimental value (63 meV/atom).[66] Though the less empirical (e.g., PBE-D3)[67] or nonempirical (e.g., vdw-DFT)[68] dispersion corrections may give a more decent description of the dispersion effect, some recent theoretical studies[69−71] demonstrated that PBE-D2 and PBE-D3 actually produce qualitatively the same and quantitatively quite close results for many periodic systems. The accuracy of the DNP basis set is comparable to that of People's 6-31G** basis set.[72] Moreover, the binding energies of the graphene/graphane and graphene/C_4H bilayers at PBE-D2/DNP (112 and 417 meV/unit cell, respectively) agree well with those obtained using the same density functional and the plane wave basis set as implemented in the VASP software package (98 and 378 meV/unit cell, respectively),[73] which indicates that the finite DNP basis set is satisfactory for the systems under investigation. Overall, our PBE-D2/DNP method is capable of dealing with the weak interactions in the systems under investigation.

Self-consistent field (SCF) calculations were performed with a convergence criterion of 10^{-6} au on the total energy and electronic computations. To ensure high-quality results, the real-space global orbital cutoff radius was chosen as high as 4.6 Å in all of the computations. We set the x and y directions parallel and the z direction perpendicular to the graphene plane and adopted a supercell length of 20 Å in the z direction. The Brillouin zone was sampled with a 6 × 6 × 1 Γ centered k points setting in geometry optimizations, and a 25 × 25 × 1 grid was used for electronic structure computations.

Because GGA typically underestimates the band gap, we also computed the band gaps using the HSE06 functional[74] and plane wave basis set as implemented in the VASP software package. HSE06 typically predicts more accurate band gaps close to experimental measurements, though it is still not the ultimate solution.[75] An accurate first-principles calculation of the band gap requires a quasi-particle correction (the GW method), which is not affordable for this work. Nevertheless, PBE and HSE06 give the same trend for the band gaps. For

dx.doi.org/10.1021/jz301821n | J. Phys. Chem. Lett. 2013, 4, 269−275

clarity, the PBE band gaps are used for discussions, while the HSE06 data are given in the Supporting Information for comparison.

■ ASSOCIATED CONTENT

Supporting Information

Band structures of graphene, graphane, and C_4H layers, charge populations of graphene in the graphene/C_4H bilayer and C_4H/graphene/C_4H trilayer, band structures of silicene and silicane layers, and the computed band gaps with HSE06 and PBE density functionals. This material is available free of charge via the Internet at http://pubs.acs.org.

■ AUTHOR INFORMATION

Corresponding Author

*E-mail: zhongfangchen@gmail.com (Z.C.).

Notes

The authors declare no competing financial interest.

■ ACKNOWLEDGMENTS

Support by the Department of Defense (Grant W911NF-12-1-0083) and NSF (Grant EPS-1010094) is gratefully acknowledged.

■ REFERENCES

(1) Chalasinski, G.; Szczesniak, M. M. State of the Art and Challenges of the Ab Initio Theory of Intermolecular Interactions. *Chem. Rev.* **2000**, *100*, 4227−4252.

(2) Meyer, E. A.; Castellano, R. K.; Diederich, F. Interactions with Aromatic Rings in Chemical and Biological Recognition. *Angew. Chem., Int. Ed.* **2003**, *42*, 1210−1250.

(3) Riley, K.; Pitoňák, M.; Juerčka, P.; Hobza, P. Stabilization and Structure Calculations for Noncovalent Interactions in Extended Molecular Systems Based on Wave Function and Density Functional Theories. *Chem. Rev.* **2010**, *110*, 5023−5063.

(4) Hobza, P. Calculations on Noncovalent Interactions and Databases of Benchmark Interaction Energies. *Acc. Chem. Res.* **2012**, *45*, 663−672.

(5) Ehrlich, S.; Moellmann, J.; Grimme, S. Dispersion-Corrected Density Functional Theory for Aromatic Interactions in Complex Systems. *Acc. Chem. Res.* **2012**, DOI: 10.1021/ar3000844.

(6) Kodama, Y.; Nishihata, K.; Nishio, M.; Nakagawa, N. Attractive Interaction between Aliphatic and Aromatic Systems. *Tetrahedron Lett.* **1977**, 2105−2108.

(7) Matsumoto, A.; Tanaka, A.; Tsubouchi, T.; Tashiro, K.; Saragai, S.; Nakamoto, S. Crystal Engineering for Topochemical Polymerization of Muconic Esters Using Halogen−Halogen and CH/π Interactions as Weak Intermolecular Interactions. *J. Am. Chem. Soc.* **2002**, *124*, 8891−8902.

(8) Kobayashi, K.; Ishii, K.; Sakamoto, S.; Shirasaka, T.; Yamaguchi, K. Guest-Induced Assembly of Tetracarboxyl-Cavitand and Tetra(3-pyridyl)-Cavitand into a Heterodimeric Capsule via Hydrogen Bonds and CH−Halogen and/or CH−π Interaction: Control of the Orientation of the Encapsulated Guest. *J. Am. Chem. Soc.* **2003**, *125*, 10615−10624.

(9) Yamamoto, Y.; Yamamoto, A.; Furuta, S.; Horie, M.; Kdama, M.; Sato, W.; Abika, K. Y.; Tsuzuki, S.; Uchimaru, T.; Hashizume, D.; et al. Synthesis and Structure of 16 π Octaalkyltetraphenylporphyrins. *J. Am. Chem. Soc.* **2005**, *127*, 14540−14541.

(10) Lakshminarayanan, P. S.; Kumar, D. K.; Ghosh, P. Solid State Structural Evidence of Chloroform−Benzene−Chloroform Adduct Trapped in Hexaanthryl Octaaminocryptand Channels. *J. Am. Chem. Soc.* **2006**, *128*, 9600−9601.

(11) Scjsteder, C. A.; Bender, S. L.; Barry, B. A. Role for Bound Water and CH−π Aromatic Interactions in Photosynthetic Electron Transfer. *J. Am. Chem. Soc.* **2005**, *127*, 7879−7890.

(12) Allen, S. E.; Mahatthananchai, J.; Bode, J. W.; Kozlowski, M. C. Oxyanion Steering and CH−π Interactions as Key Elements in an N-Heterocyclic Carbene-Catalyzed [4 + 2] Cycloaddition. *J. Am. Chem. Soc.* **2012**, *134*, 12098−12103.

(13) Harigai, M.; Kataoka, M.; Imamoto, Y. A Single CH/π Weak Hydrogen Bond Governs Stability and the Photocycle of the Photoactive Yellow Protein. *J. Am. Chem. Soc.* **2006**, *128*, 10646−10647.

(14) Lucas, R.; Gómez-Pinto, I.; Aviñó, A.; Reina, J. J.; Eritja, R.; González, C.; Morales, J. C. Highly Polar Carbohydrates Stack onto DNA Duplexes via CH/π Interactions. *J. Am. Chem. Soc.* **2011**, *133*, 1909−1916.

(15) Ganguly, H. K.; Majumder, B.; Chattopadhyay, S.; Chakrabarti, P.; Basu, G. Direct Evidence for CH···π Interaction Mediated Stabilization of Pro-*cis*Pro Bond in Peptides with Pro-Pro-Aromatic Motifs. *J. Am. Chem. Soc.* **2012**, *134*, 4661−4669.

(16) Nishio, M. CH/π Hydrogen Bonds in Organic Reactions. *Tetrahedron* **2005**, *61*, 6923−6950.

(17) Tsuzuki, S.; Honda, K.; Uchimaru, T.; Mikami, M.; Tanabe, K. The Magnitude of the CH/π Interaction between Benzene and Some Model Hydrocarbons. *J. Am. Chem. Soc.* **2000**, *122*, 3746−3753.

(18) Tsuzuki, S.; Honda, K.; Uchimaru, T.; Mikami, M.; Tanabe, K. Origin of the Attraction and Directionality of the NH/π Interaction: Comparison with OH/π and CH/π Interactions. *J. Am. Chem. Soc.* **2000**, *122*, 11450−11458.

(19) Zhao, C.; Parrish, R. M.; Smith, M. D.; Pellechia, P. J.; Sherrill, C. D.; Shimizu, K. D. Do Deuteriums Form Stronger CH−π Interactions? *J. Am. Chem. Soc.* **2012**, *134*, 14306−14309.

(20) Tsuzuki, S. CH/π Interactions. *Annu. Rep. Prog. Chem., Sect. C: Phys. Chem.* **2012**, *108*, 69−95.

(21) Bloom, J. W. G.; Raju, R. K.; Wheeler, S. E. Physical Nature of Substituent Effects in XH/π Interactions. *J. Chem. Theory Comput.* **2012**, *8*, 3167−3174.

(22) Umezawa, Y.; Tsuboyama, S.; Honda, K.; Uzawa, J.; Nishio, M. CH/π Interactions in the Crystal Structure of Organic Compounds. A Database Study. *Bull. Chem. Soc. Jpn.* **1998**, *71*, 1207−1213.

(23) Novoselov, K. S.; Geim, A. K.; Morozov, S. V.; Jiang, D.; Zhang, Y.; Dubonos, S. V.; Gregorieva, I. V.; Firsov, A. A. Electric Field Effect in Atomically Thin Carbon Films. *Science* **2004**, *306*, 666−669.

(24) Novoselov, K. S.; Falko, V. I.; Colombo, L.; Gellert, P. R.; Schwab, M. G.; Kim, P. A Roadmap for Graphene. *Nature* **2012**, *490*, 192−200.

(25) Georgakilas, V.; Otyepka, M.; Bourlinos, A. B.; Chandra, V.; Kim, N.; Kemp, K. C.; Hobza, P.; Zboril, R.; Kim, K. S. Functionalization of Graphene: Covalent and Non-Covalent Approaches, Derivatives and Applications. *Chem. Rev.* **2012**, *112*, 6156−6214.

(26) Novoselov, K. S.; Geim, A. K.; Morozov, S. V.; Jiang, D.; Khotkevich, I. V.; Gregorieva, I. V.; Dubonos, S. V.; Firsov, A. A. Two-Dimensional Gas of Massless Dirac Fermions in Graphene. *Nature* **2005**, *438*, 197−200.

(27) Novoselov, K. S; Jiang, Z.; Zhang, Y.; Morozov, S. V.; Stormer, H. L.; Zeitler, U.; Maan, J. C.; Boebinger, G. S.; Kim, P.; Geim, A. K. Room-Temperature Quantum Hall Effect in Graphene. *Science* **2007**, *315*, 1379.

(28) Lee, C. G.; Wei, X. D.; Kysar, J. W.; Hone, J. Measurement of the Elastic Properties and Intrinsic Strength of Monolayer Graphene. *Science* **2008**, *321*, 385−388.

(29) Morozov, S. V.; Novoselov, K. S.; Katsnelson, M. I.; Schedin, F.; Elias, D.; Jaszczak, J. A.; Geim, A. K. Giant Intrinsic Carrier Mobilities in Graphene and Its Bilayer. *Phys. Rev. Lett.* **2008**, *100*, 016602.

(30) Kim, K.; Choi, J. Y.; Kim, T.; Cho, S. H.; Chung, H. J. A Role for Graphene in Silicon-Based Semiconductor Devices. *Nature* **2011**, *479*, 338−344.

(31) Gyunea, F.; Katsnelson, M. I.; Geim, A. K. Energy Gaps and a Zero-Field Quantum Hall Effect in Graphene by Strain Engineering. *Nat. Phys.* **2010**, *6*, 30−33.

(32) Zhang, Y. B.; Tang, T. T.; Girit, C.; Zhao, H.; Martin, M. C.; Zettl, A.; Crommie, M. F.; Shen, Y. R.; Wang, F. Direct Observation of

a Widely Tunable Bandgap in Bilayer Graphene. *Nature* **2009**, *459*, 820−823.
(33) Elias, D. C.; Nair, R. R.; Mohiuddin, T. M. G.; Morozov, S. V.; Blake, P.; Halsall, M. P.; Ferrari, A. C.; Boukhvalov, D. W.; Katsnelson, M. I.; Geim, A. K.; et al. Control of Graphene's Properties by Reversible Hydrogenation: Evidence for Graphane. *Science* **2009**, *323*, 610−613.
(34) Haberer, D.; Guusca, C. E.; Wang, Y.; Sachdev, H.; Fedorov, A. V.; Farjam, M.; Jafari, S. A.; Vyalikh, D. V.; Usachov, D.; Liu, X. J.; et al. A. Evidence for A New Two-Dimensional C_4H-Type Polymer Based on Hydrogenated Graphene. *Adv. Mater.* **2011**, *23*, 4497−4503.
(35) Sluiter, M. H.; Kawazoe, Y. Cluster Expansion Method for Adsorption: Application to Hydrogen Chemisorption on Graphene. *Phys. Rev. B* **2003**, *68*, 085410.
(36) Sofo, J. O.; Chaudhari, A. S.; Barber, G. D. Graphane: A Two-Dimensional Hydrocarbon. *Phys. Rev. B* **2007**, *75*, 153401.
(37) Lin, Y.; Ding, F.; Yakobson, B. I. Hydrogen Storage by Spillover on Graphene as a Phase Nucleation Process. *Phys. Rev. B* **2008**, *78*, 041402(R).
(38) Singh, A. K.; Yakobson, B. I. Electronics and Magnetism of Patterned Graphene Nanoroads. *Nano Lett.* **2009**, *9*, 1540−1543.
(39) Li, Y.; Chen, Z. Patterned Partially Hydrogenated Graphene (C_4H) and Its One-Dimensional Analogues: A Computational Study. *J. Phys. Chem. C* **2012**, *116*, 4526−4534.
(40) Fokin, A. A.; Gerbig, D.; Schriner, P. R. σ/σ- and π/π-Interactions Are Equally Important: Multilayered Graphanes. *J. Am. Chem. Soc.* **2011**, *133*, 20036−20039.
(41) Janowski, T.; Pulay, P. A Benchmark Comparison of σ/σ and π/π Dispersion: The Dimers of Naphthalene and Decalin, and Coronene and Perhydrocoronene. *J. Am. Chem. Soc.* **2012**, *134*, 17520−17525.
(42) Li, Y.; Li, F.; Chen, Z. Graphane/Fluorographene Bilayer: Considerable C−H···F−C Hydrogen Bonding and Effective Band Structure Engineering. *J. Am. Chem. Soc.* **2012**, *134*, 11269−11275.
(43) Ramasubramaniam, A.; Naveh, D.; Towe, E. Tunable Band Gaps in Bilayer Graphene-BN Heterostructures. *Nano Lett.* **2011**, *11*, 1070−1075.
(44) Du, A.; Sanvito, S.; Li, Z.; Wang, D.; Jiao, Y.; Liao, T.; Sun, Q.; Ng, Y. H.; Zhu, Z.; Amal, R.; Smith, S. C. Hybrid Graphene and Graphitic Carbon Nitride Nanocomposite: Gap Opening, Electron−Hole Puddle, Interfacial Charge Transfer, and Enhanced Visible Light Response. *J. Am. Chem. Soc.* **2012**, *134*, 4393−4397.
(45) Cracium, M. F.; Russo, S.; Yamamoto, M.; Oostinga, J. B.; Morpurgo, A. F.; Tarucha, S. Trilayer Graphene Is a Semimetal with a Gate-Tunable Band Overlap. *Nat. Nanotechnol.* **2009**, *4*, 383−388 , and references therein.
(46) Oostinga, J. B.; Heersche, H. B.; Liu, X. L.; Morpurgo, A. F.; Vanersypen, L. M. K. Gate-Induced Insulating State in Bilayer Graphene Devices. *Nat. Mater.* **2008**, *7*, 151−157.
(47) Zhu, L.; Wang, J.; Ding, F. Robust Electronic Properties of Sealed Graphene for Electronic Applications. *J. Phys. Chem. C* **2012**, *116*, 8027−8033.
(48) Takeda, K.; Shiraishi, K. Theoretical Possibility of Stage Corrugation in Si and Ge Analogs of Graphite. *Phys. Rev. B* **1994**, *50*, 14916−14922.
(49) Lalmi, B.; Oughaddou, H.; Enriquez, H.; Kara, A.; Vizzini, S.; Ealet, B.; Aufray, B. Epitaxial Growth of A Silicene Sheet. *Appl. Phys. Lett.* **2010**, *97*, 223109.
(50) Vogt, P.; Padova, P. D.; Quaresima, C.; Avila, J.; Frantzeskakis, E.; Asensio, M. C.; Resta, A.; Ealet, B.; Lay, G. L. Silicene: Compelling Experimental Evidence for Graphenelike Two-Dimensional Silicon. *Phys. Rev. Lett.* **2012**, *108*, 155501.
(51) Feng, B. J.; Ding, Z.; Meng, S.; Yao, Y.; He, X.; Cheng, P.; Chen, L.; Wu, K. Evidence of Silicene in Honeycomb Structures of Silicon on Ag(111). *Nano Lett.* **2012**, *12*, 3507−3511.
(52) Fleurence, A.; Friedlein, R.; Ozaki, T.; Kawai, H.; Wang, Y.; Yamada-Takamura, Y. Experimental Evidence for Epitaxial Silicene on Diboride Thin Films. *Phys. Rev. Lett.* **2012**, *108*, 245501.
(53) Yamanaka, S.; Matsu-ura, H.; Ishikawa, M. New Deintercalation Reaction of Calcium from Calcium Disilicide. Synthesis of Layered Polysilane. *Mater. Res. Bull.* **1996**, *31*, 307−316.
(54) Okamoto, H.; Kumai, Y.; Sugiyama, Y.; Mitsuoka, T.; Nakanishi, K.; Ohta, T.; Nozaki, H.; Yamaguchi, S.; Shirai, S.; Nakano, H. Silicon Nanosheets and Their Self-Assembled Regular Stacking Structure. *J. Am. Chem. Soc.* **2010**, *132*, 2710−2718.
(55) Nakano, H.; Nakano, M.; Nakanishi, K.; Tanaka, D.; Sugiyama, Y. Preparation of Alkyl-Modified Silicon Nanosheets by Hydrosilylation. *J. Am. Chem. Soc.* **2012**, *134*, 5452−5455.
(56) Cahangirov, S.; Topsakal, M.; Akturk, E.; Sahin, H.; Ciraci, S. Two- and One-Dimensional Honeycomb Structures of Silicon and Germanium. *Phys. Rev. Lett.* **2009**, *102*, 236804.
(57) O'Hare, A.; Kusmartsev, F. V.; Kugel, K. I. A Stable "Flat" Form of Two-Dimensional Crystals: Could Graphene, Silicene, Germanene Be Minigap Semiconductors? *Nano Lett.* **2012**, *12*, 1045−1052.
(58) Houssa, M.; Scalise, E.; Sankaran, K.; Pourtois, G.; Afanas'ev, V. V.; Stesmans, A. Electronic Properties of Hydrogenated Silicene and Germanene. *Appl. Phys. Lett.* **2011**, *98*, 223107.
(59) Osborn, T. H.; Farajian, A. A.; Pupysheva, O. V.; Aga, R. S.; Lew Yan Voon, L. C. Ab Initio Simulations of Silicene Hydrogenation. *Chem. Phys. Lett.* **2011**, *511*, 101−105.
(60) Lew Yan Voon, L. C.; Sandberg, E.; Aga, R. S.; Farajian, A. A. Hydrogenated Compounds of Group-IV Nanosheets. *Appl. Phys. Lett.* **2010**, *97*, 163114.
(61) Ni, Z.; Liu, Q.; Tang, K.; Zheng, J.; Zhou, J.; Qin, R.; Gao, Z.; Yu, D.; Lu, J. Tunable Bandgap in Silicene and Germanene. *Nano Lett.* **2012**, *12*, 113−118.
(62) Delley, B. An All-electron Numerical Method for Solving the Local Density Functional for Polyatomic Molecules. *J. Chem. Phys.* **1990**, *92*, 508−517.
(63) Delley, B. From Molecules to Solids with the DMol3 Approach. *J. Chem. Phys.* **2000**, *113*, 7756−7764.
(64) Perdew, J. P.; Burke, K.; Ernzerhof, M. Generalized Gradient Approximation Made Simple. *Phys. Rev. Lett.* **1996**, *77*, 3865−3868.
(65) Grimme, S. Semiempirical GGA-Type Density Functional Constructed with a Long-Rang Dispersion Correction. *J. Comput. Chem.* **2007**, *27*, 1787−1799.
(66) Zacharia, R.; Ulbricht, H.; Hertel, T. Interlayer Cohensive Energy of Graphite from Thermal Desorption of Polyaromatic Hydrocarbons. *Phys. Rev. B* **2004**, *69*, 155406.
(67) Grimme, S.; Antony, J.; Ehrlich, S.; Krieg, H.. A Consistent and Accurate ab initio Parametrization of Density Functional Dispersion Correction (DFT-D) for the 94 Elements H−Pu. *J. Chem. Phys.* **2010**, *132*, 154104.
(68) Dion, M.; Rydberg, H.; Schröder, E.; Langreth, D. C.; Lundqvist, B. I. Van der Waals Density Functional for General Geometries. *Phys. Rev. Lett.* **2004**, *92*, 246401.
(69) Moellmann, J.; Grimme, S. Importance of London Dispersion Effects for the Packing of Molecular Crystals: A Case Study for Intramolecular Stacking in a Bis-thiophene Derivative. *Phys. Chem. Chem. Phys.* **2010**, *12*, 8500−8504.
(70) Ehrlich, S.; Moellmann, J.; Reckien, W.; Bredow, T.; Grimme, S. System-Dependent Dispersion Coefficients for the DFT-D3 Treatment of Adsorption Processes on Ionic Surfaces. *ChemPhysChem* **2011**, *12*, 3414−3420.
(71) Reckien, W.; Jantzko, F.; Peintinger, M.; Bredow, T. Implementation of Empirical Dispersion Corrections to Density Functional Theory for Periodic Systems. *J. Comput. Chem.* **2012**, *33*, 2023−2031.
(72) Hehre, W. J.; Radom, L.; Schlyer, P. v. R.; Pople, J. A. *Ab Initio Molecular Orbital Theory*; Wiley: New York, 1986.
(73) Kresse, G.; Hafner, J. Ab Initio Molecular Dynamics for Liquid Metals. *Phys. Rev. B* **1993**, *47*, 558−561.
(74) Barone, V.; Hod, O.; Peralta, J. E.; Scuseria, G. E. Accurate Prediction of the Electronic Properties of Low-Dimensional Graphene Derivatives Using a Screened Hybrid Density Functional. *Acc. Chem. Res.* **2011**, *44*, 269−279.

(75) Jain, M.; Chelikowsky, J. R.; Louie, S. G. Reliability of Hybrid Functionals in Predicting Band Gaps. *Phys. Rev. Lett.* **2011**, *107*, 216806.